

LARGE-SCALE SOFT X-RAY LOOPS AND THEIR MAGNETIC CHIRALITY IN BOTH HEMISPHERES

HONGQI ZHANG¹, SHANGBIN YANG¹, YU GAO¹, JIANGTAO SU¹, D. D. SOKOLOFF^{1,2}, AND K. KUZANYAN^{1,3}

¹ Key Laboratory of Solar Activity, National Astronomical Observatories, Chinese Academy of Sciences, Beijing 100012, China; hzhang@bao.ac.cn

² Department of Physics, Moscow State University, Moscow 119992, Russia

³ IZMIRAN, Troitsk, Moscow Region 142190, Russia

Received 2010 March 29; accepted 2010 June 29; published 2010 August 4

ABSTRACT

The magnetic chirality in the solar atmosphere has been studied based on soft X-ray and magnetic field observations. It is found that some of the large-scale twisted soft X-ray loop systems occur for several months in the solar atmosphere, before the disappearance of the corresponding background large-scale magnetic field. This paper provides observational evidence of the helicity of the large-scale magnetic field in the solar atmosphere and the reverse one relative to the helicity rule in both hemispheres with solar cycles. The transfer of the magnetic helicity from the subatmosphere is consistent with the formation of large-scale twisted soft X-ray loops in both the solar hemispheres.

Key words: Sun: activity – Sun: corona – Sun: magnetic topology

Online-only material: color figures

1. INTRODUCTION

Magnetic helicity plays an important role in solar flares and coronal mass ejections (CMEs), and in the dynamo processes that cause the 11 year solar cycle (Zhang & Low 2005). Magnetic helicity is an integral quantity reflecting the global complexity of the magnetic field. It can be inferred in several ways based on the measurements of the magnetic field in the solar atmosphere. The pioneering study of magnetic helicity was taken by some authors based on the accumulation of magnetic helicity $H_m = \int \mathbf{A} \cdot \mathbf{B} d^3x$ in the solar atmosphere (e.g., Berger & Field 1984; Chae 2001) and on the mean factor of force-free field $\overline{\alpha_{ff}} = \overline{(\nabla \times \mathbf{B})_{\perp} \cdot \mathbf{B}_{\perp} / B_{\perp}^2}$ (or the mean current helicity $\overline{h_c} = \overline{(\nabla \times \mathbf{B})_{\perp} \cdot \mathbf{B}_{\perp}}$) in solar active regions (e.g., Seehafer 1990).

It is found that the mean current helicity in most solar active regions in the northern (southern) hemisphere tend to show a negative (positive) sign. This trans-equatorial sign rule for magnetic chirality was first discovered by Hale et al. (1919) from the $H\alpha$ pattern of active regions. A series of studies on the hemispheric sign rule for magnetic helicity have been presented in recent years (Seehafer 1990; Pevtsov et al. 1995; Abramenko et al. 1996; Bao & Zhang 1998; Hagino & Sakurai 2005). The reversed sign of current helicity in solar active regions with respect to the trans-equatorial sign rule, which is found in high correlation with the powerful solar flare–CMEs, has been noticed. Bao et al. (1999), Zhang et al. (2000), Liu & Zhang (2002), and Wang et al. (2004) found that the active regions with reversed signs of current helicity show a higher possibility of releasing magnetic energy into the interplanetary space than regular ones do.

Statistical analysis of the observed current helicity in active regions with solar cycles has been presented by Bao & Zhang (1998), Zhang & Bao (1999), Bao et al. (2000), Hagino & Sakurai (2005), and Xu et al. (2007). It was found that the mean helicity of solar active regions changes with the phase of solar cycles and the mean sign of helicity occurs reversed from the hemispheric rule in some phases of solar cycles. Several mechanisms of magnetic helicity generation inside the Sun have been proposed (Longcope et al. 1998; Berger & Ruzmaikin 2000; Kleeorin et al. 2003; Blackman & Brandenburg 2003;

Sokoloff et al. 2006; Zhang et al. 2006). In comparison with observational results, the mirror symmetrical reversal of the magnetic helicity of solar active regions relative to the preferred hemispheric trends at the different phases of a solar cycle have been theoretically demonstrated (Choudhuri et al. 2004; Xu et al. 2009). A similar simulation for the distribution of current helicity in the full-Sun has been provided by Yeates et al. (2009).

Recently, the distribution of the current helicity of solar active regions with solar cycle phases and latitude has been presented by Zhang et al. (2010) based on the vector magnetograms of active regions for more than 20 years of observations at Huairou Solar Observing Station. This distribution shows the following observational evidence: electric current helicity and twist follow the propagation of the magnetic activity dynamo waves recorded by sunspots. The helicity and twist oscillate with 11 year periods like sunspots, rather than 22 year periods as magnetic fields do. The helicity and twist patterns are, in general, anti-symmetric with respect to the solar equator. The helicity pattern is more complicated than Hale’s polarity law for sunspots. Areas of the “wrong” sign have been found at the ends of the butterfly wings as well as at their very beginnings. The average amplitude of the helicity does not show any significant dependence on the solar cycle phase. The maximum value of helicity, at the surface at least, seems to occur near the edges of the butterfly diagram of sunspots.

Using photospheric vector magnetograms from the Haleakala Stokes Polarimeter and coronal X-ray images from the *Yohkoh* Soft X-Ray Telescope (SXT), Pevtsov et al. (1997) inferred values of the force-free field parameter α at both photospheric and coronal levels within 140 active regions. They found that both values are well correlated. Both values are poorly correlated only for active regions in which both signs of alpha are represented well and in which their method of analysis therefore breaks down. This implies that the helical coronal configuration of soft X-ray loops provides basic information on the magnetic helicity in the solar atmosphere. It is also a considerable parameter to analyze the distribution of the hemispheric sign of magnetic helicity and its evolution with the solar cycle.

In this paper, we present the distribution of the sign of magnetic helicity inferred from the distribution of soft X-ray

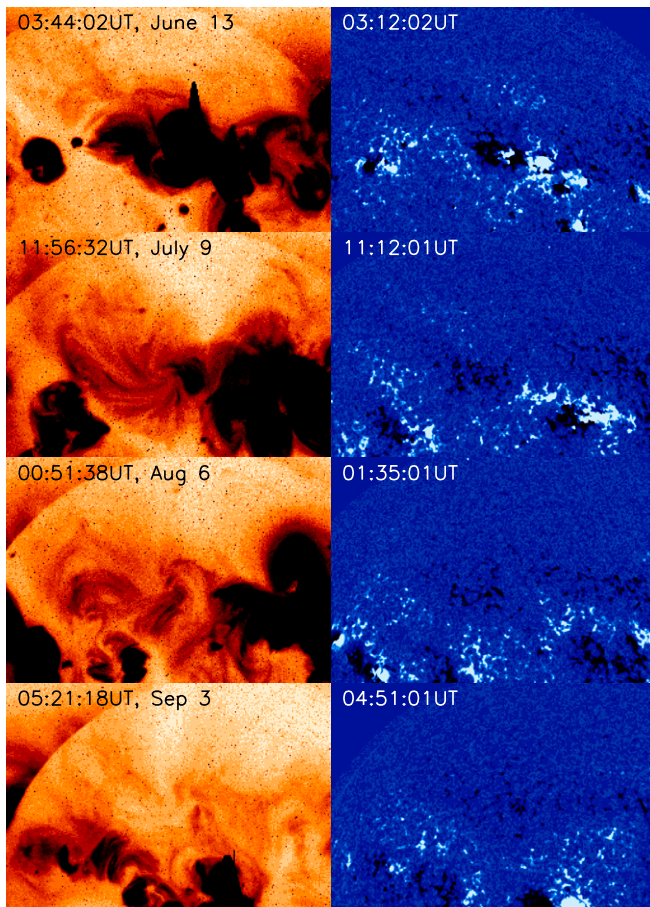


Figure 1. Soft X-ray images of a part of the Sun (left), where the large-scale soft X-ray loops twist clockwise, and the corresponding photospheric magnetograms (right) in the period of 2000 June–September. The white (black) color indicates the positive (negative) polarity in the magnetograms. The top is north and the right is west.

(A color version of this figure is available in the online journal.)

loops and its evolution with solar cycles. We also discuss the large-scale reversal magnetic helicity in both hemispheres in some phase of the solar cycle and analyze its relevance in the framework of the solar dynamo.

2. MAGNETIC CHIRALITY OF SOFT X-RAY LOOPS RELATED TO SOLAR ACTIVE REGIONS

Figure 1 shows a sample of the twisted large-scale soft X-ray configuration in the solar northern hemisphere from the *Yohkoh* SXT. It is found that the twisted large-scale soft X-ray configuration remained in the solar atmosphere for several months in the period of 2000 June–September, even though the topology of the soft X-ray configuration gradually changed. It is normally believed that the soft X-ray configuration in the solar atmosphere provides basic information of the magnetic field, as it is believed that the field is bound up in the ionized plasma. This large-scale twisted magnetic field in the solar atmosphere originated from a decaying solar active region NOAA 9033 in 2000 June. This means that the twisted magnetic field in the solar atmosphere originated from solar active regions and the diffused remainder of the helical magnetic field from the active regions can be kept for a long time in the solar atmosphere (Zhang 2006). The twist of soft X-ray loops in the left-handedness in the solar northern hemisphere is consistent with the handed rule of magnetic helicity presented by some authors in recent years

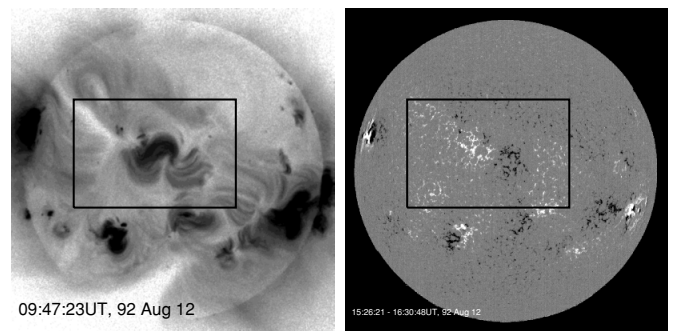


Figure 2. Full-disk soft X-ray image of the Sun (left) and the corresponding photospheric magnetogram (right) on 1992 August 12. The white (black) color indicates the positive (negative) polarity in the magnetogram. The top is north and the right is west.

(Seehafer 1990; Pevtsov et al. 1995; Abramenko et al. 1996; Bao & Zhang 1998; Hagino & Sakurai 2005).

Figure 2 shows the full-disk soft X-ray images of the Sun and the corresponding photospheric magnetograms on 1992 August 12. It is found that the right(left)-handed chirality of the large-scale soft X-ray loops occurred near the center of the solar disk in the northern (southern) hemisphere. This means that the handedness of these soft X-ray loops is opposite to the statistical handedness rule for magnetic helicity. Figure 3 shows a series of soft X-ray images of a part of the Sun (left), where the large-scale soft X-ray loops twist counterclockwise, and also shows the corresponding photospheric magnetograms (right) in the period of 1992 June–October. This region is marked by boxes in Figure 2. The counterclockwise chirality does not change with evolution of the soft X-ray configuration. This means that the sign of helicity holds for a relatively long period in the solar atmosphere. This is also consistent with the results reported by Zhang & Bao (1999) that the reverse helicity of solar active regions tends to occur in some specific longitudes and holds its sign for several solar rotations.

Figures 4 and 5 show the other two examples of some notable handedness of soft X-ray loops in both the hemispheres, marked by boxes. Figure 4 shows that the right-handedness (positive helicity) of the large-scale soft X-ray loops occurs in the northern hemisphere, while Figure 5 shows that the left-handedness (negative helicity) of the large-scale soft X-ray loops occurs in the southern hemisphere. These large-scale soft X-ray loops are connected with the enhanced network of magnetic fields and active regions.

3. HEMISPHERIC DISTRIBUTION OF HELICAL SOFT X-RAY LOOPS

To analyze the distribution of magnetic chirality in the solar atmosphere, in Table 1 we present statistics on the 753 large-scale soft X-ray loop systems in the period of 1991–2001 observed by the *Yohkoh* satellite. The handedness of soft X-ray loops can be inferred by their twist or sigmoid configuration. It is found that the handedness of soft X-ray loops statistically obeys the hemispheric sign rule. Most of them possess left (right)-handedness in the northern (southern) hemisphere. It is found that the handedness for about 31% of soft X-ray loops cannot be identified because their configurations are not too far from the approximation of the potential field or cannot be clearly identified as sigmoid or twist configurations. This lack of identification does not significantly influence the trend in the ratio of the handednesses of soft X-ray loops between the

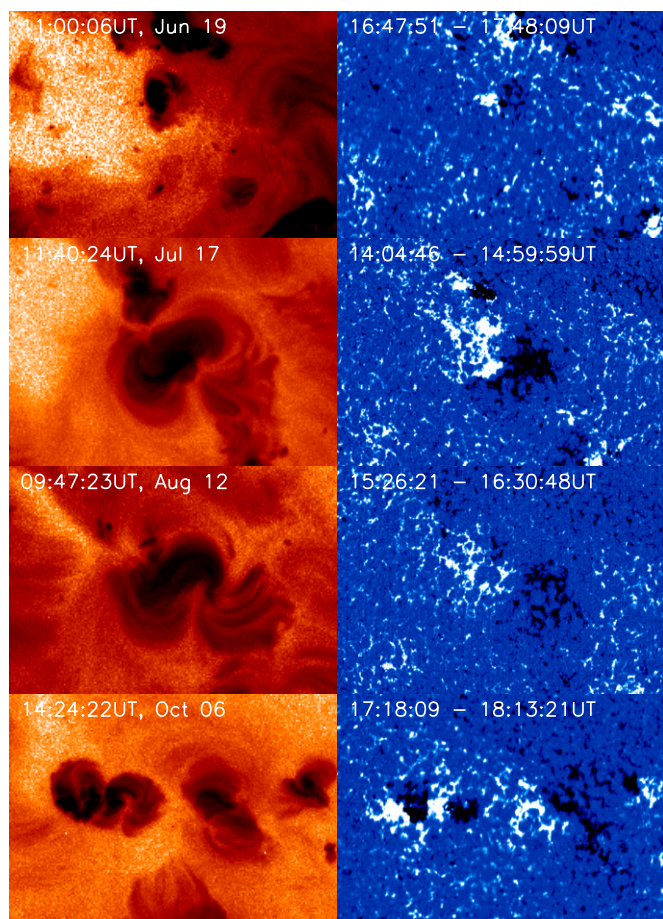


Figure 3. Soft X-ray images of a part of the Sun (left), where the large-scale soft X-ray loops twist counterclockwise, and the corresponding photospheric magnetograms (right) in the period of 1992 June–October. The white (black) colors indicate the positive (negative) polarity in the magnetograms. (A color version of this figure is available in the online journal.)

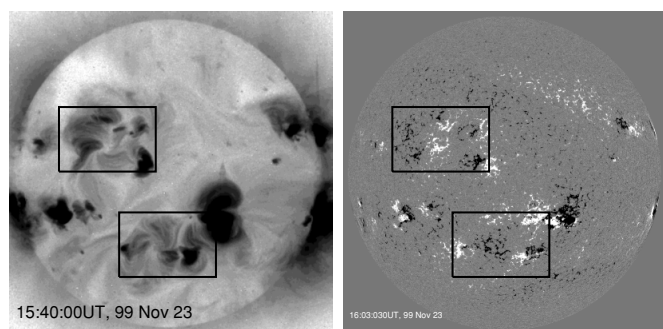


Figure 4. Full-disk soft X-ray image of the Sun (left) and the corresponding photospheric magnetogram (right) on 1999 November 23. The white (black) color indicates the positive (negative) polarity in the magnetogram. The top is north and the right is west.

northern and southern hemispheres. As these unidentified soft X-ray loop systems are ignored, one will find that the portion of the systems that are in accord with the hemispheric rule is 77.3% in the northern hemisphere and 81.5% in the southern hemisphere. This is roughly consistent with results calculated from the vector magnetograms (Pevtsov et al. 1995; Bao & Zhang 1998; Hagino & Sakurai 2005; Zhang et al. 2010).

Figure 6 shows the proportion of soft X-ray loops following the hemispheric handedness rule for helicity in the northern and southern hemispheres. The change of the proportion of

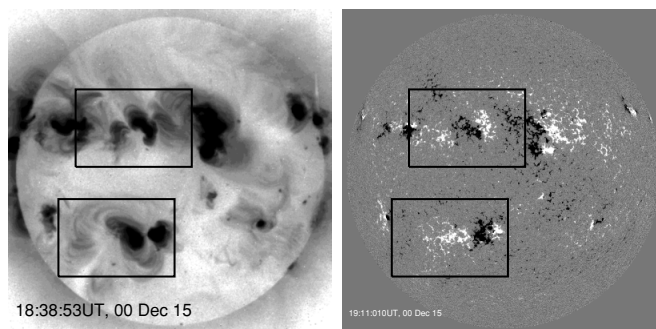


Figure 5. Full-disk soft X-ray image of the Sun (left) and the corresponding photospheric magnetogram (right) on 2000 December 15. The white (black) color indicates the positive (negative) polarity in the magnetogram. The top is north and the right is west.

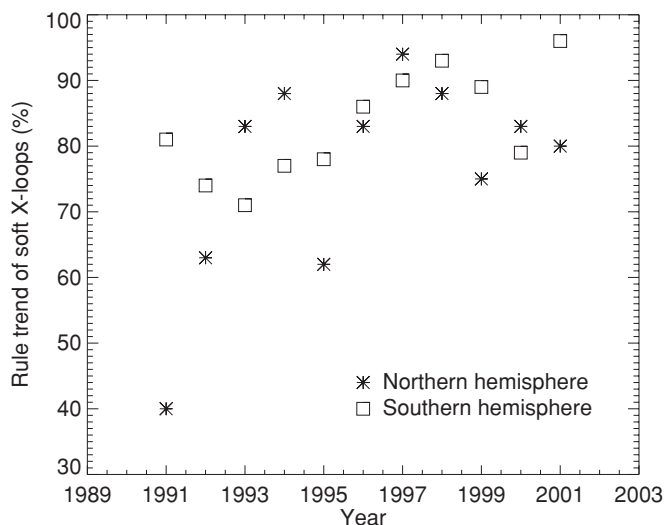


Figure 6. Proportion of soft X-ray loops following the hemispheric handedness rule of helicity in the northern and southern hemispheres.

soft X-ray loops following the hemispheric handedness rule of helicity and their imbalance of chirality in both hemispheres is also found. The relative high tendency of reverse magnetic helicity has occurred in 1991, 1992, and 1995 in the northern hemisphere, while it has not been significant in the southern hemisphere. This is consistent with the results shown in Figures 2 and 3.

Figure 7 shows the statistical latitudinal distribution of soft X-ray loops in Figure 6. It is found that the trends of the mean latitude of soft X-ray loops migrate toward the equator with the solar cycle phase following sunspots in the butterfly diagram. Because there were very few soft X-ray loops in 1991, 1995, and 1996 included in our statistics, the deviation from the butterfly diagram in these years can be noted. Most of the large-scale soft X-ray loops show the left(right)-handedness in the northern (southern) hemisphere, which follows the handedness rule for the current helicity of solar active regions, while the statistical distribution of the reverse soft X-ray loops shows left(right)-handedness in the southern (northern) hemisphere, as one can see in Figure 7.

4. HANDEDNESS OF THE LARGE-SCALE SOFT X-RAY LOOPS AND THE MAGNETIC (CURRENT) HELICITY

It has been noted that the synthetic analysis on the accumulation of magnetic helicity as well as the relationship with

Table 1
Statistics of Handedness of Soft X-ray Loops in the Northern and Southern Hemispheres

3 Year	1991	1992	1993	1994	1995	1996	1997	1998	1999	2000	2001	Total
N_n	4	38	25	31	5	5	16	23	32	24	22	225
P_n	6	24	5	4	3	1	2	3	9	6	5	68
Q_n	7	27	22	14	5	5	11	15	18	13	7	144
P_s	13	23	24	13	7	6	19	26	16	11	27	185
N_s	7	8	10	4	2	1	2	2	2	3	1	42
Q_s	3	12	4	5	7	4	5	22	14	6	7	89
Total	40	132	90	71	29	22	55	91	91	63	69	753

Notes. N is the number of soft X-ray loops with left-handedness. P is the number of soft X-ray loops with right-handedness. Q is the number of unidentified soft X-ray loops. The subscript n and s indicate the northern and southern hemispheres, respectively.

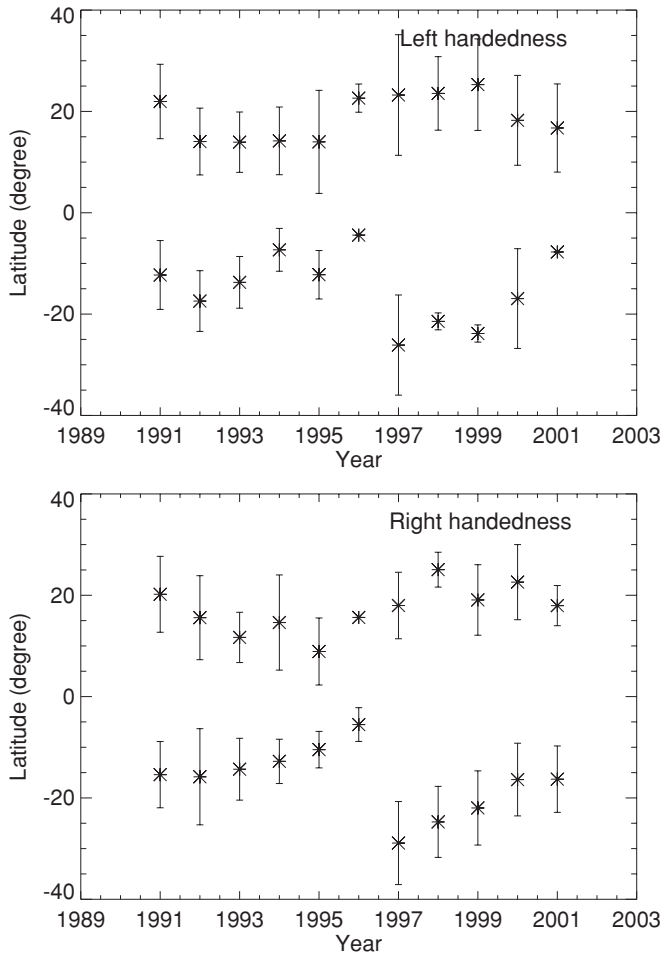


Figure 7. Mean latitudinal distribution of soft X-ray loops with the left- and right-handedness. σ -error bars are shown by vertical lines.

mean current helicity density (and also mean force-free α) is an important way to understand the basic information on dynamics of magnetic helicity in solar active regions (Zhang 2006). It can be used to analyze the relationship between the handedness of large-scale soft X-ray loops and the corresponding magnetic helicity in the solar atmosphere, while the helicity of large-scale soft X-ray loops is probably due to the nearby solar active regions and enhanced networks.

Figure 8 shows the rate of change and accumulation of magnetic helicity inferred by MDI magnetograms relative to the large-scale soft X-ray loop region of Figure 1. The accumulation of magnetic helicity has been calculated using the local

Table 2
Mean Current Helicity Density and α Parameter Inferred from Vector Magnetograms of Active Regions Observed at Huairou Relative to Figure 1

Date	AR	Lat (deg)	$\overline{h_c}(10^{-2}G^2/m)$	$\overline{\alpha}(10^{-7}/m)$
2000 Jun 12–15	9033	15.8	-0.329	-0.209
2000 Jul 6	9070	10.1	-0.184	-0.413
2000 Aug 9–11	9114	10.3	-0.085	-0.125
2000 Aug 31–Sep 6	9149	6.7	-0.059	-0.113

correlative tracking (LCT) method (Chae 2001) as the regions are located near the center of the solar disk. Over all of the time intervals, the accumulation of magnetic helicity has been found to monotonically increase with time of negative helicity transfer from the subatmosphere to the corona. The accumulated helicity was $-13.5 \times 10^{42} \text{ Mx}^2$ on 2000 June 9–13, $-19.9 \times 10^{42} \text{ Mx}^2$ on 2000 July 7–19, $-1.59 \times 10^{42} \text{ Mx}^2$ on 2000 August 5–6, and $-9.74 \times 10^{42} \text{ Mx}^2$ on 2000 September 1–3. The average accumulation of magnetic helicity per day is $-3.60 \times 10^{42} \text{ Mx}^2$. Because the contribution of the September data is disregarded due to the evanescence of the large-scale twisted soft X-ray loops, the average accumulation of magnetic helicity is $-3.63 \times 10^{42} \text{ Mx}^2$ per day. It can be estimated that an order of $-4 \times 10^{44} \text{ Mx}^2$ magnetic helicity has been transferred into the corona and contributed to the large-scale soft X-ray loops in the period of 2000 June–September.

Table 2 shows the mean current helicity density and force-free α parameter of solar active regions calculated by vector magnetograms observed at Huairou Solar Observing Station, National Astronomical Observatory of China. These active regions show the negative sign of current helicity, and they have the same sign with accumulated magnetic helicity. Active region NOAA 9033 was a fast developing active region on 2000 June 13 as shown in the right panel of Figure 1, it was NOAA 9070 in the next solar rotation, and became the large-scale enhanced magnetic network in the magnetogram of August 6. Active region NOAA 9114 located in the left of the magnetogram on August 6 and active region NOAA 9149 located near the bottom right on September 3 are shown in Figure 1. It can be estimated that the large-scale soft X-ray loops are mainly due to active region NOAA 9033 and its following rotated regions in the solar disk, while the contribution from other active regions, such as NOAA9114 and 9149, also probably cannot be neglected. This shows the consistency between the accumulation of magnetic helicity and the remaining handedness of the magnetic field in the solar atmosphere.

Table 3 shows the mean current helicity density and force-free α parameter of corresponding active regions in the target region

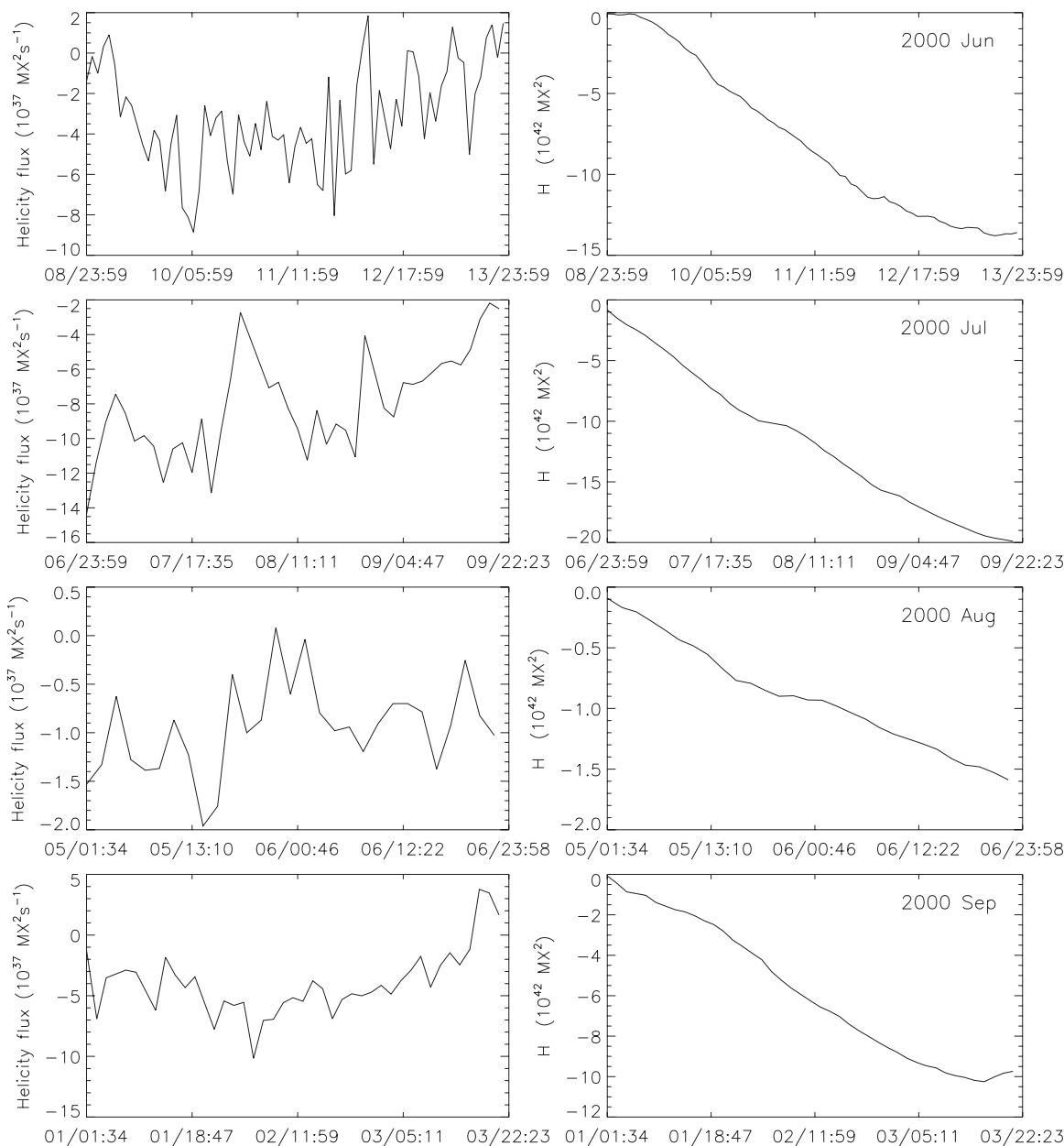


Figure 8. Injection rate (left) and accumulation (right) of magnetic helicity in the regions of Figure 1.

of Figure 3, which are inferred from vector magnetograms at the Huairou Solar Observing Station and the National Astronomical Observatory of Japan. The positive sign of these helicity parameters is consistent with the right-handedness of the large-scale soft X-ray loops in Figure 3.

A similar case of the same sign of the magnetic helicity of solar active regions in the northern and southern hemispheres can be found in 2003 October and November. These active regions produced a notable amount of unexpected eruptive events (Zhang et al. 2003; Berlicki et al. 2006; Guo et al. 2006; Li et al. 2006; Mandrini et al. 2006; Uddin et al. 2006; Zanna et al. 2006). Liu & Zhang (2006) found that about $-6 \times 10^{43} \text{ Mx}^2$ magnetic helicity was transported from the subatmosphere into the corona in AR 10488 (L288, N8) in 2003 October 26–31. AR 10486 (L293, S15) formed in the southern hemisphere. Zhang et al. (2008) detected the $-5 \times 10^{43} \text{ Mx}^2$ magnetic helicity from the active region AR 10486 with the strong counterclockwise rotation of sunspots in 2003 October 25–30. The mean current

helicity of these active regions shows a negative sign. This provides interesting observational evidence that one sign of magnetic helicity occurs in the whole of the Sun. It means that the hemispheric sign rule can be disobeyed in some periods of the solar cycle. It is also consistent with the synthetic analysis of the magnetic field in these active regions by Zhou et al. (2007). This finding can be confronted with the account of the total magnetic helicity injection over the whole solar cycle presented by Georgoulis et al. (2009).

Figures 9 and 10 show the rate of change and accumulation of magnetic helicity inferred by MDI magnetograms relative to the large-scale soft X-ray loop region in Figures 4 and 5, and also the corresponding contribution in the solar disk in the previous solar rotation. The accumulation of magnetic helicity is calculated as the target regions are located near the center of the solar disk. It is found that the accumulation process of magnetic helicity in these regions is more complex than that of monotone variation in Figures 1 and 3.

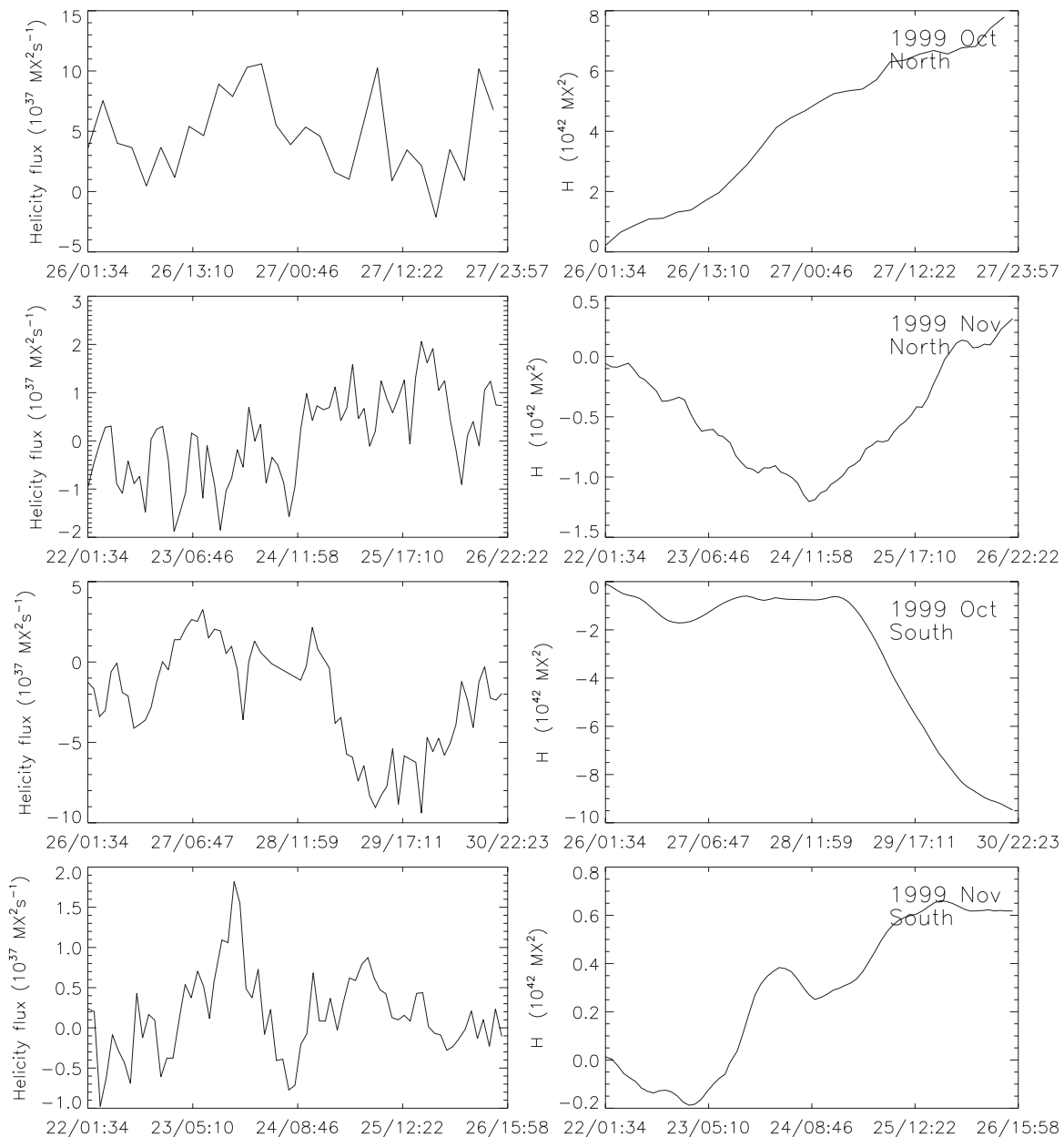


Figure 9. Injection rate (left) and accumulation (right) of magnetic helicity in the regions of both hemispheres marked by boxes in Figure 4.

Figure 9 shows the basic accumulation of positive magnetic helicity in the previous solar rotation of the target region in the northern hemisphere ($8 \times 10^{42} \text{ Mx}^2$ transports on 1999 October 26–27), even if there is a change in sign of accumulated magnetic helicity on November 22–24, while the increase of positive helicity in the target region of the southern hemisphere occurred on November 23–25.

Figure 10 shows about $-8.9 \times 10^{42} \text{ Mx}^2$ magnetic helicity accumulated in the previous solar rotation of the target region on 2000 November 16–21 in the southern hemisphere, even if about $1.87 \times 10^{43} \text{ Mx}^2$ helicity had accumulated on 2000 December 16–18. Figure 10 also shows that, in the northern hemisphere, the accumulated helicity was about $-1.4 \times 10^{41} \text{ Mx}^2$ on 2000 November 16–18 and $-1.1 \times 10^{43} \text{ Mx}^2$ on 2000 December 14–18.

Table 4 displays the mean current helicity density and force-free α parameter of corresponding target active regions in Figure 5 and the region in the southern hemisphere in

the previous solar rotation, which are inferred from vector magnetograms at the Huairou Solar Observing Station. It is found that the mean current helicity parameters show a negative sign inferred from vector magnetograms in active region NOAA 9231 on 2000 November 17 and a positive sign in the corresponding region NOAA 9264 in the next solar rotation on 2000 December 15. Upon comparison with Figure 10, it is found that the sign difference of mean current helicity parameters is consistent with the accumulation of magnetic helicity in the target regions in Figure 5. This means that the formation of reverse handedness of the large-scale soft X-ray loops is contributed by the transfer of magnetic helicity from the subatmosphere and is a relatively complex process.

5. DISCUSSION

In this paper, we have demonstrated the large-scale soft X-ray loops visible in soft X-ray images and their relationship

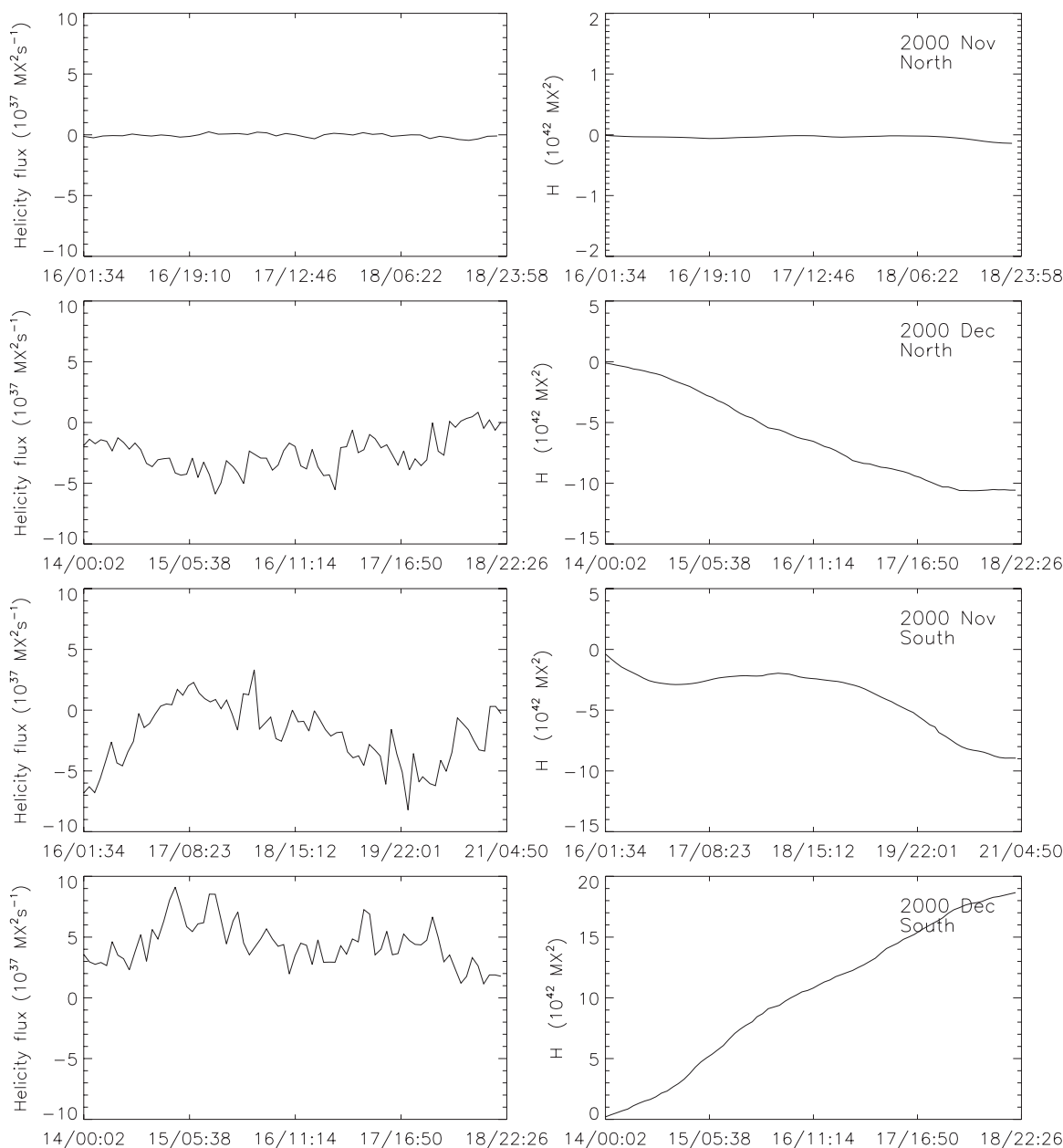


Figure 10. Injection rate (left) and accumulation (right) of magnetic helicity in the regions of both hemispheres marked by boxes in Figure 5.

Table 3

Mean Current Helicity Density and α Parameter Inferred from Vector Magnetograms of Active Regions Observed at Huairou and Mitaka Relative to Figure 3

Date	AR	Time (UT)	Lat (deg)	Lon (deg)	$\bar{h}_c(10^{-2}G^2/m)$	$\bar{\alpha}(10^{-7}/m)$
1992 Jun 24	7201	02:48:30	18.3	47.7	1.591	0.683
1992 Jul	7227	...				
1992 Aug 10 (<i>J</i>)	EH	01:23:31	24.4	-36.8	0.366	0.228
1992 Oct	7299	...				

Note. *J* is inferred by the vector magnetogram on 1992 August 10 observed at the National Astronomical Observatory of Japan in Mitaka and *EH* indicates the enhanced network.

Table 4

Mean Current Helicity Density and α Parameter Inferred from Vector Magnetograms of Active Regions Observed at Huairou Relative to Figure 5

Hemisphere	Date	AR	Time (UT)	Lat (deg)	Lon (deg)	$\bar{h}_c(10^{-2}G^2/m)$	$\bar{\alpha}(10^{-7}/m)$
North	2000 Nov	No					
North	2000 Dec 15	9272	03:39:29	20.9	-18.9	-0.0248	-0.101
South	2000 Nov 17	9231		-29.3	-33.3	-0.138	-0.128
South	2000 Dec 15	9264		-30.8	-15.9	0.0797	0.0993

with magnetic helicity. Thereby, we have presented examples that show that the magnetic chirality holds the same handedness with transfer upward from the subatmosphere. It is consistent with the morphologically same handedness of soft X-ray loops in both hemispheres as shown in Figures 2–5. Furthermore, we have demonstrated examples of the statistical imbalance in the opposite handedness of soft X-ray loops and magnetic helicity in some phases of solar cycles (such as in 1992 June–October and 2003 October–November). Thus, we have simultaneously observed the cases of the same sign of magnetic helicity across the equator, contrary to the usual occurrence of the opposite sign.

The large-scale soft X-ray loops are connected with solar active regions and enhanced magnetic networks, and we have shown the statistical relation of their handedness with the hemispheric rule for helicity in both hemispheres. In some years, such as in 1997 and 1998 in our statistical analysis, this correlation appears very high. The fraction of the soft X-ray loops following the hemispheric rule is slightly different from that of the current helicity inferred from vector magnetograms (e.g., Pevtsov et al. 1995; Bao & Zhang 1998; Hagino & Sakurai 2005; Zhang et al. 2010), due to the difference in the nature of this parameter, while it may also provide some message on the mechanism that generates the magnetic field in the subatmosphere and the reversal of the helicity of the magnetic field in the solar atmosphere at some latitudes and periods of the solar cycle.

The statistical distribution of the mean current helicity density of solar active regions presented in Figure 2 of Zhang et al. (2010) shows evidence of the imbalance of helicity in the decaying phase of solar cycles 22 and 23. One can see domains in latitude and time of reversed sign with respect to the statistical hemispheric rule at the beginning as well as at the end of the butterfly wings. This is consistent with our results, although we focus on morphological and statistical analysis of the handedness of the large-scale soft X-ray loops of active regions and enhanced networks. We propose this phenomenon as the penetration of the activity wave from one hemisphere into the other one, a sort of trespassing into the “wrong” hemisphere with respect to the average sign of helicity.

The magnetic helicity can be considered a measure of the mirror asymmetry of solar magnetic fields. They are generated, according to the mean-field solar dynamo model, due to the effects of solar differential rotation and the action of Coriolis force on turbulent motions of plasma in the solar convection zone (e.g., Berger & Ruzmaikin 2000; Kuzanyan et al. 2000; Kleorin et al. 2003; Choudhuri 2003; Choudhuri et al. 2004; Zhang et al. 2006). However, the issue of the occurrence of the same sign components of magnetic helicity in both hemispheres has not been studied sufficiently.

The Sun is an open system for magnetic helicity. The eruption of flare–CMEs brings magnetic helicity from the solar atmosphere into the interplanetary space (Zhang & Low 2005), which probably causes the imbalance of remaining magnetic helicity in the convection zone in both hemispheres. Due to the eruption process, the balance of helicity in both hemispheres can be seriously distorted even if the dynamo and turbulent convection mechanisms produce helicity of opposite sign across the equator and absolute amounts of helicity are comparable. This imbalance of helicity can be compensated for by the large-scale helicity transport from one hemisphere to another one. The possible agent of such transfer could be the trans-equatorial magnetic field inside the solar convection zone.

Within the framework of the solar dynamo model, we can interpret the trans-equatorial interaction of dynamo waves as a proxy of global modulation of the solar activity such as the Gleissberg cycle. However, simple one-dimensional models of magnetic field interaction across the equator (such as, e.g., Galitskii et al. 2005) can hardly interact effectively enough for quantitatively realistic times, which for the Gleissberg cycle is of order 100 yr. Hereby, we may suggest an additional mechanism of the interaction of dynamo waves across the equator by means of the transfer of twist and helicity, which may occur more effectively than a mechanism of the magnetic field itself. For future studies, we may also suggest investigating such a possible mechanism of interaction at atmospheric and subatmospheric levels in the Sun, probably by means of Alfvénic waves.

Further development of the mechanism on the generation of local magnetic helicity in the convection zone, as well as the global evolution of helicity with the solar cycle and its parts which are symmetric and anti-symmetric with respect to the equator, still remains a challenge for theory.

For forthcoming studies of basic properties of the solar dynamo, the symmetric and anti-symmetric parts of the magnetic helicity of solar active regions in both hemispheres and their evolution with the solar cycle still need to be observationally confirmed in detail.

The authors thank Prof. Arnab Rai Choudhuri for his comments and suggestions on the manuscript. This study is supported by National Basic Research Program of China grant 2006CB806301, National Natural Science Foundation (NNSF) of China grants 1061120338, 10473016, 10673016, 60673158, 10733020, and Important Directional Project of Chinese Academy of Sciences grant KLCX2-YW-T04. This work has been carried out within the framework of the joint Chinese–Russian collaborative project. We acknowledge support from the NNSF of China and the Russian Foundation for Basic Research under grants 08-02-92211 and 10-02-00960-a. K.K. and D.S. thank the Visiting Professorship program of the Chinese Academy of Sciences and the National Astronomical Observatories of China for support of their visits to Beijing.

REFERENCES

- Abramenko, V. I., Wang, T. J., & Yurchishin, V. B. 1996, *Sol. Phys.*, **168**, 75
 Bao, S. D., Ai, G. X., & Zhang, H. Q. 2000, *JA&A*, **21**, 303
 Bao, S. D., & Zhang, H. Q. 1998, *ApJ*, **496**, L43
 Bao, S., Zhang, H., Ai, G., & Zhang, M. 1999, *A&AS*, **139**, 311
 Berger, M., & Field, G. 1984, *J. Fluid Mech.*, **147**, 133
 Berger, M., & Ruzmaikin, A. 2000, *J. Geophys. Res.*, **105**, 10481
 Berlicki, A., Mein, P., & Schmieder, B. 2006, *A&A*, **445**, 1127
 Blackman, E., & Brandenburg, A. 2003, *ApJ*, **584**, L99
 Chae, J. 2001, *ApJ*, **560**, L95
 Choudhuri, A. 2003, *Sol. Phys.*, **215**, 31
 Choudhuri, A., Chatterjee, P., & Nandy, D. 2004, *ApJ*, **615**, L57
 Galitskii, V., Sokoloff, D., & Kuzanyan, K. 2005, *Astron. Rep.*, **49**, 337
 Georgoulis, M. K., Rust, D. M., Pevtsov, A. A., Bernasconi, P. N., & Kuzanyan, K. M. 2009, *ApJ*, **705**, L48
 Guo, J., Zhang, H., Chumak, O., & Liu, Y. 2006, *Sol. Phys.*, **237**, 25
 Hagino, M., & Sakurai, T. 2005, *PASJ*, **57**, 481
 Hale, G. E., Ellerman, F., Nicholsin, S. B., & Joy, A. H. 1919, *ApJ*, **49**, 153
 Kleorin, N., Kuzanyan, K., Moss, D., Rogachevskii, I., Sokoloff, D., & Zhang, H. 2003, *A&A*, **409**, 1097
 Kuzanyan, K., Bao, S., & Zhang, H. 2000, *Sol. Phys.*, **191**, 231
 Li, H., Schmieder, B., Aulanier, G., & Berlicki, A. 2006, *Sol. Phys.*, **237**, 85
 Liu, J., & Zhang, H. 2006, *Sol. Phys.*, **234**, 21
 Liu, Y., & Zhang, H. 2002, *A&A*, **386**, 656
 Longcope, D., Fisher, G., & Pevtsov, A. 1998, *ApJ*, **507**, 417
 Mandrini, C. H., Demoulin, P., Schmieder, B., Deluca, E. E., Pariat, E., & Uddin, W. 2006, *Sol. Phys.*, **238**, 293

- Pevtsov, A., Canfield, R., & McClymont, A. 1997, *ApJ*, **481**, 973
- Pevtsov, A. A., Canfield, R. C., & Metcalf, T. R. 1995, *ApJ*, **440**, L109
- Seehafer, N. 1990, *Sol. Phys.*, **125**, 219S
- Sokoloff, D., Bao, S., Kleorin, N., Kuzanyan, K., Moss, D., Rogachevskii, I., Tomin, D., & Zhang, H. 2006, *Astron. Nachr.*, **327**, 876
- Uddin, W., Chandra, R., & Ali, S. 2006, *JA&A*, **27**, 255
- Wang, J., Zhou, G., & Zhang, J. 2004, *ApJ*, **615**, 1021
- Xu, H., Gao, Y., Popova, E. P., Nefedov, S. N., Zhang, H., & Sokoloff, D. D. 2009, *Astron. Rep.*, **53**, 160
- Xu, H., Gao, Y., Zhang, H., Sakurai, T., Pevtsov, A. A., & Sokoloff, D. 2007, *Adv. Space Res.*, **39**, 1715
- Yeates, A. R., Mackay, D. H., & van Ballegooijen, A. A. 2009, *ApJ*, **680**, L165
- Zanna, G., Schmieder, B., Mason, H., Berlicki, A., & Bradshaw, S. 2006, *Sol. Phys.*, **239**, 173
- Zhang, H. 2006, *Chin. J. Astron. Astrophys.*, **6**, 96
- Zhang, H., & Bao, S. 1999, *ApJ*, **519**, 876
- Zhang, H., Sakurai, T., Pevtsov, A., Gao, Y., Xu, H., Sokoloff, D., & Kuzanyan, K. 2010, *MNRAS*, **402**, L30
- Zhang, H., Sakurai, T., Shibata, K., Shimojo, M., & Kurokawa, H. 2000, *A&A*, **357**, 725
- Zhang, H., Sokoloff, D., Rogachevskii, I., Moss, D., Kuzanyan, K., & Kleorin, N. 2006, *MNRAS*, **365**, 276
- Zhang, H., et al. 2003, *Chin. J. Astron. Astrophys.*, **3**, 491
- Zhang, M., & Low, B. 2005, *ARA&A*, **43**, 103
- Zhang, Y., Zhang, M., & Zhang, H. 2008, *Sol. Phys.*, **250**, 75
- Zhou, G., Wang, J., Wang, Y., & Zhang, Y. 2007, *Sol. Phys.*, **244**, 13